A VARIABLE STRUCTURE APPROACH TO FORCE/MOTION CONTROL OF ROBOT MANIPULATORS

UN APPROCCIO A STRUTTURA VARIABILE PER IL CONTROLLO DELLA FORZA E DEL MOTO DI MANIPOLATORI ROBOTICI

A.Balestrino, A.Bicchi, A.Landi and D.Prattichizzo

D.S.E.A , Università di Pisa
via Diotisalvi 2, 56126 Pisa, Italy

Abstract

A strategy for force/motion control of a manipulator in contact with its environment is presented. The automatical exploration of unknown objects in order to reconstruct their geometrical features from sensed information is considered. The hybrid controller employs a computed-torque scheme in order to realize force regulation. The design of the velocity loop is approached with a variable structure technique. Numerical examples of a planar three link robot moving along constraint surfaces are presented for illustration.

1 Introduction

In many robotic applications, including grinding, contour following, deburring, scribing, assembling, etc., the manipulator is brought in contact with a constraint surface. The problem of determining the input torques to achieve trajectory tracking on the surface with specified constraint forces, is known as constrained robot control (CRC). The CRC problem is closely related to research in compliant control [1-3] and force feedback control [4-6]. An example of CRC is the automatical exploration of unknown objects by means of a dextrous robotic hand [7-8]. CRC techniques can be distinguished in impedance control methods [1-2] that do not use force sensor feedback information and hybrid techniques involving explicit force control, based on available force sensing at the contact. The hybrid control method [9-11] is based on the partition of the control action into a force control subspace, usually normal to the constraint surface, and into a position control subspace along the tangential direction. A lot of advanced methods have been presented, such as nonlinear decoupling control [12], adaptive control [13-16], computed torque control [17], learning techniques [18-19], to cite a few. Other simple and easily implementable regulators, with low sensitivity to external disturbances and parametric variations, are based on sliding mode techniques [20]. However applications of the latter type of controllers in CRC tasks have not been adequately exploited.

In this paper, a particular contour following problem is addressed, that is the automatical exploration of a rigid and unknown surface with friction in order to reconstruct its geometric features from sensed information. To achieve this objective the controller has to continuously regulate both the normal contact force to preserve the contact with the object and the tangential velocity to generate the motion of the sensorized fingertip along the object surface.

The force control loop is realized via a computed torque technique based on a simple contact model. Similarly to the works of Eppinger and Goldenberg [21-22] in a one degree of freedom model, the contact model is based on a set of "virtual springs" between the robot and the object at the contact point. In the work of Goldenberg [21], computed torque technique is presented as a particular effective state feedback reducing the steady state force error to zero.

The design of the velocity loop is approached with a variable structure technique, such that a velocity error signal is added to the tangential force reference with an automatic hierarchy in this control action: the velocity loop becomes effective only when the normal contact force approaches the reference value. In the classical hybrid control scheme proposed by Raibert and Craig [9] such hierarchy was achieved by assigning different time constants to the force control loop and to the velocity control loop.

The paper is organized as follows: in Section 2 the dynamical model of the robot exploring an object is introduced. In Section 3 the synthesis of the force controller is derived and its stability is proved. In Section 4 the hybrid force/velocity controller and the variable structure logic controller is developed. In Section 5 simulation results are shown. The conclusions are presented in Section 6.

2 Dynamical Model of the Robot Exploring an Object

Consider the system comprised of a robot (i.e., a simple chain of links connected by revolute or prismatic joints), and from an object to be explored. Suppose that the object is fixed in the "base" frame B. This system could describe for instance a robotic hand grasping an object and exploring its contour by means of a single finger. We suppose that the end-effector touches the object at point c and that the contact force and torque exerted on the object at the contact point is $\bar{t} = (p^T, m^T)^T \in \mathbb{R}^6$. Let $q \in \mathbb{R}^q$ be a vector of generalized coordinates, completely describing the configuration of the robot and let $c \in \mathbb{R}^3$ be the vector describing the contact point in the base frame.

To incorporate contact constraint in the model, relative displacements between the object and the end-effector at the contact point must be considered. Therefore, we introduce the reference frames ${}^oC$ fixed with respect to the object and centered in c, the location of the contact point, and the reference frames ${}^mC$ fixed with respect to the last link and centered in c. The differential kinematics is

$$ {}^m\dot{x} = \bar{J}\,\dot{q}, \qquad (1)$$

where

$$ {}^m\dot{x} = ({}^m\dot{c}^T, {}^m\dot{\phi}^T)^T. $$

and the matrix $\bar{J}$ ($\in \mathbb{R}^{6\times q}$) is the end-effector jacobian relating the end-effector velocity ${}^m\dot{x}$ with the joint velocity ${}^m\dot{q}$.

Contact constraint imposes that some components of the relative displacement ${}^ox - {}^mx$ are influenced by reaction forces, depending upon the type of contact. Among the contact models describing the interaction between the robot finger and the object, the hard and the soft finger model [23] are probably the most common. Contact constraint can be expressed in terms of a suitable selection matrix $H \in \mathbb{R}^{t\times 6}$,

$$ H({}^mx - {}^ox) = 0. \qquad (2)$$

For the hard finger contact model, it holds

$$ H = \begin{pmatrix} I_3 & O_3 \end{pmatrix}, \qquad (3)$$

while for the soft finger contact model we have

$$ H = \begin{pmatrix} I_3 & O_{3\times 3} \\ n_c{}^T & O_{1\times 3} \end{pmatrix}, \qquad (4)$$

where n_c is the unit normal vector at the contact point c.

A set of "virtual springs" interposed between the links and the object at the contact points are introduced to model contact interactions. The elastic relationship between the relevant components of the relative displacements ${}^ox - {}^mx$ and the corresponding components of contact force can be written as

$$ t = KH({}^mx - {}^ox). \qquad (5)$$

where $t \in \mathbb{R}^t$ is related to $\bar{t} \in \mathbb{R}^6$ by

$$ \bar{t} = H^T t. \qquad (6)$$

The components of t are only those contact forces and torques that are relevant to contact description. The stiffness matrix $K \in \mathbb{R}^{t\times t}$ incorporates the structural elasticity of the object and of the robot. As a consequence of its physical nature, K can be assumed non-singular. A detailed and comprehensive study on the evaluation and the realization of desirable stiffness matrices with articulated hands has been presented by Cutkosky and Kao [24].

Robot dynamics interacts with the object by means of the vector of forces and torques $\bar{t}$ exerted on the object. Let the vector $\tau \in \mathbb{R}^q$ be the joint actuator torques, the dynamical description of the system can be derived using Lagrange's equations:

$$ M(q)\ddot{q} + Q(q,\dot{q}) + \bar{J}^T\bar{t} = \tau \qquad (7)$$

where

$$Q(q,\dot{q}) = C(q,\dot{q})\dot{q} + v(q). \quad (8)$$

The hand inertia matrix $M(q)$ is symmetric and positive definite and the Q term include velocity dependent forces and gravity forces. From (6) we obtain,

$$\begin{aligned} M(q)\ddot{q} + Q(q,\dot{q}) + \bar{J}^T H^T t = \tau \\ M(q)\ddot{q} + Q(q,\dot{q}) + J^T t = \tau \end{aligned} \quad (9)$$

where J is defined as

$$J = H\bar{J} \in \mathbb{R}^{t \times q}. \quad (10)$$

3 Force Control

In this section a computed torque method based on the virtual spring model of the contact interaction is proposed. The following hypothesis are assumed

- the overall stiffness of the system K is lumped in the force sensor, while the surface is supposed rigid. The effect of the object stiffness, joint elasticity and sensor compliance on the stability of the force control loop for 1 DOF systems have been studied in [21].
- $\bar{J}$ is invertible.
- the sensorized fingertip is supposed to have infinite curvature (point-finger).
- ${}^m x$ represents the position of the finger end-point as calculated by the rigid kinematics of the robot. When contact occurs, ${}^m x$ is a virtual position of the finger end-point inside the object surface.
- ${}^o x$ is the actual position of the contact point, as it is measured by the tactile sensor.

Differentiating the forward kinematics,

$$\ddot{q} = \bar{J}^{-1}({}^m\ddot{x} - \dot{\bar{J}}\dot{q}), \quad (11)$$

by substituting (11) into (9) we obtain

$$M\bar{J}^{-1m}\ddot{x} - M\bar{J}^{-1}\dot{\bar{J}}\dot{q} + C\dot{q} + v + J^T t = \tau. \quad (12)$$

Choosing a control law in the form:

$$\tau = -M\bar{J}^{-1}\dot{\bar{J}}\dot{q} + C\dot{q} + v + \tau_a, \quad (13)$$

the dynamics (12) becomes

$$M\bar{J}^{-1m}\ddot{x} + J^T t = \tau_a. \quad (14)$$

Designing a PD-controller with feed-forward compensation as follows

$$\tau_a = J^T((K_p - I)e_f + K_d\dot{e}_f + t_d) + \tau_b, \quad (15)$$

where $e_f = t_d - t$ is the force error between the desired force t_d and the measured one t, while K_p and K_d are definite positive matrices, then, premultipling by KH, we get:

$$KH^m\ddot{x} = KH\bar{J}M^{-1}\bar{J}^T H^T(K_p e_f + K_d\dot{e}_f) + KH\bar{J}M^{-1}\tau_b. \quad (16)$$

Finally the control law τ_b is choosen,

$$\tau_b = M\bar{J}^{-1o}\ddot{x} + M(KH\bar{J})^+\ddot{t}_d, \quad (17)$$

where $(KH\bar{J})^+$ is the pseudoinverse of the matrix $KH\bar{J} \in \mathbb{R}^{t\times q}$. In the hypothesis of time invariance of the matrix KH, we have

$$\ddot{t} = KH({}^m\ddot{x} - {}^o\ddot{x})$$

and the force error dynamics results,

$$\ddot{e}_f + KH\bar{J}M^{-1}\bar{J}^T H^T (K_p e_f + K_d \dot{e}_f) = 0 \tag{18}$$

Being $K > 0$ and the jacobian $\bar{J}$ not singular, $H\bar{J}M^{-1}\bar{J}^T H^T$ is definite positive. Then the dynamic evolution of force error is given by

$$\ddot{e}_f + B\dot{e}_f + Ce_f = 0 \tag{19}$$

with $B, C > 0$.
Therefore the total control law

$$\tau = -M\bar{J}^{-1}\dot{\bar{J}}\dot{q} + C\dot{q} + v + J^T((K_p - I)e_f + K_d\dot{e}_f + t_d) + M\bar{J}^{-1}\,{}^{o}\ddot{x} + M(KH\bar{J})^R \ddot{t}_d, \tag{20}$$

guarantees that the force error tends asymptotically to zero.

From (18) it can be remarked that the error dynamics depends on the matrices $\bar{J}$ and M, i.e. on the manipulator posture. In order to avoid this dependence a compensating controller could be adopted in the form

$$\begin{aligned} K_p &= (H\bar{J}M^{-1}\bar{J}^T H^T)^{-1} K^{-1} K_p' \\ K_d &= (H\bar{J}M^{-1}\bar{J}^T H^T)^{-1} K^{-1} K_d' \end{aligned} \tag{21}$$

thus the error dynamics results

$$\ddot{e}_f + K_d'\dot{e}_f + K_p' e_f = 0 \tag{22}$$

where K_p' e K_d' are suitable time invariant definite positive matrices and the error becomes independent from the manipulator posture.

4 Force/Velocity Control for Sensorial Exploration of Objects

The goal of the sensorial exploration is the extraction of useful surface features: e.g. properties relating to the surface geometry, friction coefficients, material compliance, etc.. This information can be used for instance during subsequent phases of the manipulation task. In this paper the problem of geometric feature extraction is approached in order to obtain a geometric characterization of objects that can be applied to the analysis of grasp stability and to manipulation planning. In the following, we assume that tactile information is available from a sensor providing:

- the position of the contact point on the fingertip surface;
- the direction of the unit vector normal to the contacting surfaces;
- the intensity and direction of the resultant contact force (comprised of both compression and friction components);
- the intensity of the torque generated by friction forces.

Such information is available for instance from sensors as those described in [27]. The control technique is based on two concurrent actions: the first consists in the continuous control of normal force, the second is a velocity control generating small motions of the fingertip along the object surface. The normal force control between the fingertip and the object guarantees contact during the sensorial exploration, while the velocity control allows displacements along the tangential direction of the contact point in order to explore the surface with a suitable policy. The tactile sensor is thus able to process tactile data and to reconstruct the geometry of the object surface being explored. The hybrid structure of the force/position controller can be seen with respect to the constraint-frame [25]: the force will be controlled along the normal direction at the contact point, while the velocity of the end-effector will be controlled along the tangent direction.

In this section a technique is considered in order to add a velocity control at the force controller described in the previous section. This task can be realized by means of a suitable construction of the reference t_d in (22).

A point contact with friction is considered, more precisely we assume that no torque is exerted between the manipulator and the object (this hypothesis is realistic for low friction, low compliance materials).

Let $\mathbf{n}_v$ and $\mathbf{t}_v$ be the normal and the tangent vectors at the contact point, respectively. The force error $\mathbf{e}_f$ can be decomposed along such directions,

$$\mathbf{e}_{fn} = (f_{dn} - f_n)\mathbf{n}_v \tag{23}$$
$$\mathbf{e}_{ft} = (f_{dt} - f_t)\mathbf{t}_v \tag{24}$$

where f_{dn} and f_{dt} are scalar values corresponding to the given normal force and tangent force reference.

In order to maintain contact with the surface, along the normal direction the set-point f_{dn} is fixed at a constant value while the force $\mathbf{f}_t = f_t \mathbf{t}_n$ along the tangential direction measured by the tactile sensor is compensated adding the compensation torque

$$\tau_f = -\mathbf{J}^T \mathbf{f}_t. \tag{25}$$

If a perfect compensation of the friction force is matched, the measured force along the tangential direction at the exploring surface becomes zero; then if the set-point reference is set to zero, the force error (24) is zero too. The technique referred to as hybrid force-velocity control uses the tangential component of the force error in order to correct the velocity error, i.e. a reference r_{dt} along the tangential direction is built in the following way:

$$r_{dt} = k_v(v_{td} - v_t)\mathbf{t}_v \tag{26}$$

where v_{dt} is the reference for tangential velocity v_t. The new reference r_{dt} has to be inserted in (24) to obtain

$$\mathbf{e}_t = [r_{dt} - f_t]\mathbf{t}_v = [k_v(v_{td} - v_t) - f_t]\mathbf{t}_v \tag{27}$$

where $\mathbf{e}_t$ is the hybrid force/velocity error along the tangential direction. Therefore the global error is given by

$$\mathbf{e} = [f_{dn} - f_n]\mathbf{n}_v + [-f_t + (k_v(v_{td} - v_t))]\mathbf{t}_v. \tag{28}$$

The error $\mathbf{e}$ has an hybrid nature, its dynamics are given by (22) and tend asymptotically to zero.
If the friction force f_t is exactly compensated by using sensor information, from (28),

$$\mathbf{e} = [f_{dn} - f_n]\mathbf{n}_v + [k_v(v_{td} - v_t)]\mathbf{t}_v, \tag{29}$$

and the orthogonality of the directions $\mathbf{n}_v$ and $\mathbf{t}_v$ guarantees that asymptotically

$$f_n = f_{dn} \tag{30}$$
$$v_t = v_{td}. \tag{31}$$

while if the friction force is not exactly compensated, from (28) a velocity steady-state error arises along the tangential direction

$$k_v(v_{td} - v_t) = f_t. \tag{32}$$

To counteract this effect a high gain proportional controller or the introduction of an integral action can be adopted.

The velocity loop ensures the motion of the fingertip along the object surface during the exploration. This action is characterized by a lower priority than that of the normal force control. In fact, to maintain a given force also in the presence of surface asperities, during the exploration, is a prioritary task with respect to a continuous movement, in order to avoid the risk of loosing contact or to crash the object. In classical hybrid control schemes [9] this priority is achieved designing the force and the velocity control loop with different time constants. We propose to insert a variable structure controller (VSC), on the velocity loop. The gain of the controller is given by a variable coefficient depending upon the normal contact force error, its design logic follows the rule:
A) $\mathbf{k}_v$ tends to zero for high force error,
B) $\mathbf{k}_v$ is active when the force error approaches the steady-state value.
Analytically, the proposed structure is

$$k_v(\mathbf{e}_{fn}) = \frac{k_v'}{1 + |c\ \mathbf{e}_{fn}|^n}. \tag{33}$$

Similar variable structure control have been presented in [26]. By means of the variable structure coefficient k_v an automatic control hierarchy is established and the velocity loop becomes effective if and only if the normal contact force exerted by the fingertip on the exploring surface is near the stationary value.
The complete force/motion control structure is reported in fig.1.

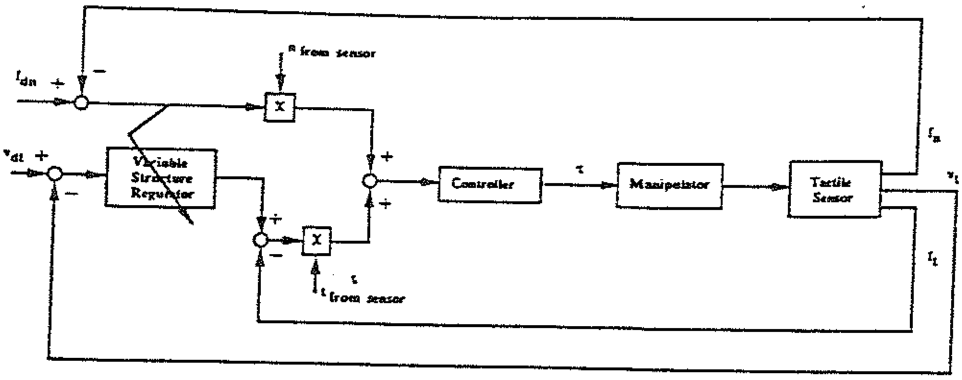

Figure 1: Force/velocity control

5 Simulations

Simulations have been executed showing the capabilities of the force/velocity control scheme. The model of the manipulator we refer to is a three link planar finger with three rotoidal joints. The fingertip is sensorized by means of a tactile sensor. The contact is described by an hard finger model. The sensor is modelled by two orthogonal springs linking the sensorized point to the last link (according to the hypothesis of sensor infinite curvature). Springs are in compression during the contact with the object and are not stressed without contact. The vector ${}^m\mathbf{x}$ represents the position of the sensorized end-point as calculated by the rigid kinematics of the robot and describes a virtual trajectory inside the object surface when the contact occurs. In our case,

$$ {}^m\mathbf{x} = \begin{pmatrix} {}^m x_1 \\ {}^m x_2 \end{pmatrix} = \begin{pmatrix} l_1 cos(q_1) + l_2 cos(q_1 + q_2) + l_3 cos(q_1 + q_2 + q_3) \\ l_1 sin(q_1) + l_2 sin(q_1 + q_2) + l_3 sin(q_1 + q_2 + q_3) \end{pmatrix} \tag{34} $$

where q_i and l_i are the joint coordinate and the length of the i-th link respectively. The actual position of the contact point is given by ${}^o\mathbf{x}$ obtained in simulation by intersecting the surface with the normal from the point ${}^m\mathbf{x}$. The equation describing analytically the surface to be explored is needed to set up the sensor model and also to compute the normal and the tangential direction. Straight lines and circumferences are the curves considered. In the following the expression of the contact point ${}^o\mathbf{x}$ and the normal and the tangential directions are reported.
In the case of a straight line in the plane (x_1, x_2) with slope a and intersection with x_1-axis in $(b, 0)$

$$ s(x_1, x_2) = x_2 - a(x_1 - b) = 0, \tag{35} $$

the contact point results

$$ {}^o\mathbf{x} = \begin{pmatrix} {}^o x_1 \\ {}^o x_2 \end{pmatrix} = \begin{pmatrix} \frac{a}{a^2+1}(ab + {}^m x_2 + \frac{{}^m x_1}{a}) \\ a(\frac{a}{a^2+1}(ab + {}^m x_2 + \frac{{}^m x_1}{a}) - b) \end{pmatrix} \tag{36} $$

and the normal and tangential directions are,

$$ \mathbf{n}_v = \frac{1}{\sqrt{a^2+1}} \begin{pmatrix} a \\ -1 \end{pmatrix} \tag{37} $$

$$ \mathbf{t}_v = \frac{1}{\sqrt{a^2+1}} \begin{pmatrix} 1 \\ a \end{pmatrix} \tag{38} $$

When the curve is the circumference with radius R and center $(c, 0)$

$$ s(x_1, x_2) = (x_1 - c)^2 + x_2^2 = R^2, \tag{39} $$

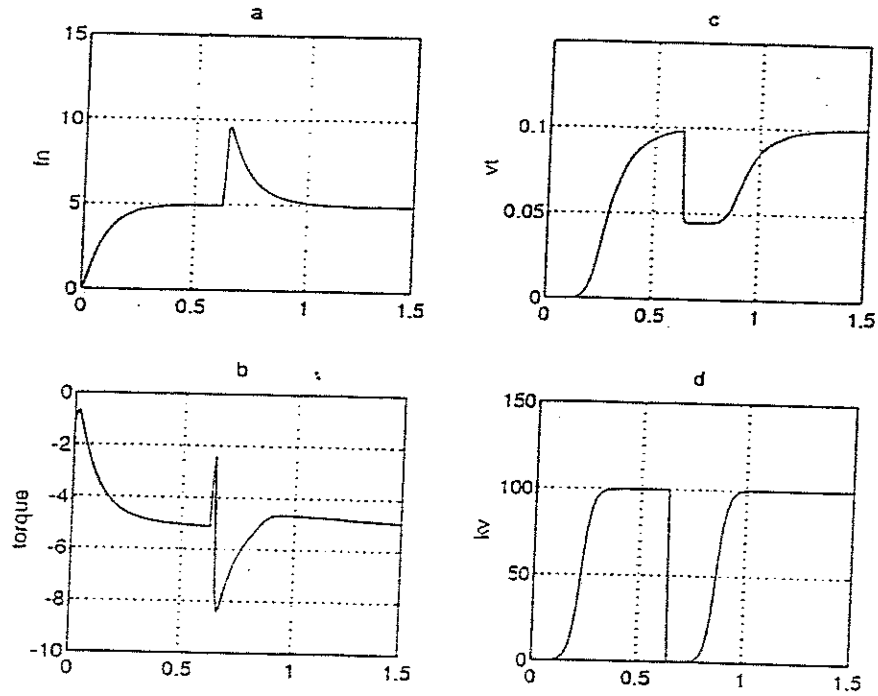

Figure 2: Straight lines exploration

the contact point results

$$ {}^o\mathbf{x} = \begin{pmatrix} {}^o x_1 \\ {}^o x_2 \end{pmatrix} = \begin{pmatrix} c - \sqrt{\frac{R^2}{G^2+1}} \\ \sqrt{R^2 - ({}^o x_1 - c)^2} \end{pmatrix} \tag{40} $$

where

$$ G = \frac{{}^m x_2}{{}^m x_1 - c} \tag{41} $$

and the normal and tangential direction are,

$$ \mathbf{n}_v = \begin{pmatrix} -\frac{{}^o x_1 - c}{R} \\ -\frac{\sqrt{R^2 - ({}^m x_1 - c)^2}}{R} \end{pmatrix} \tag{42} $$

$$ \mathbf{t}_v = \begin{pmatrix} \frac{\sqrt{R^2 - ({}^m x_1 - c)^2}}{R} \\ -\frac{{}^o x_1 - c}{R} \end{pmatrix} \tag{43} $$

Let K be a diagonal matrix with diagonal element $K(i,i) = k_s$ representing the sensor stiffness matrix K. The force measured by the sensor is

$$ \mathbf{f} = -\mathbf{K}({}^o\mathbf{x} - {}^m\mathbf{x}). \tag{44} $$

Friction force is supposed exactly compensated.

In the first simulation the explored surface is a piecewise straight line with slope $a_1 = 1$ and $a_2 = 2$ (fig.3a); the sensor stiffness is supposed to be $k_s = 10^4 N/m$, and each link is supposed to be of length $l_i = 1m$ and having mass $m_i = 1kg$. The initial condition of the robot dynamics is characterized by a null joint velocity and by an initial posture such that the contact with surface occurs with null normal force. The controller used is that reported in (20) and (21). The matrix K'_p and K'_d are diagonal with equal diagonal elements $k'_p = 1000$ and $k'_d = 100$. The variable structure controller is chosen as follows

$$ k_v = \frac{100}{1 + |2\, e_{fn}|^4}. \tag{45} $$

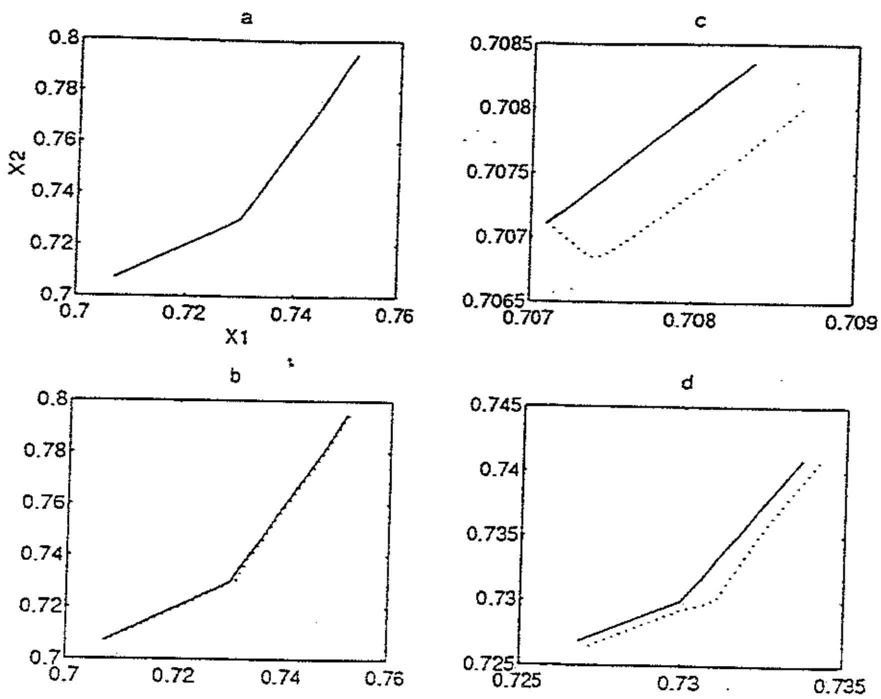

Figure 3: Straight lines exploration

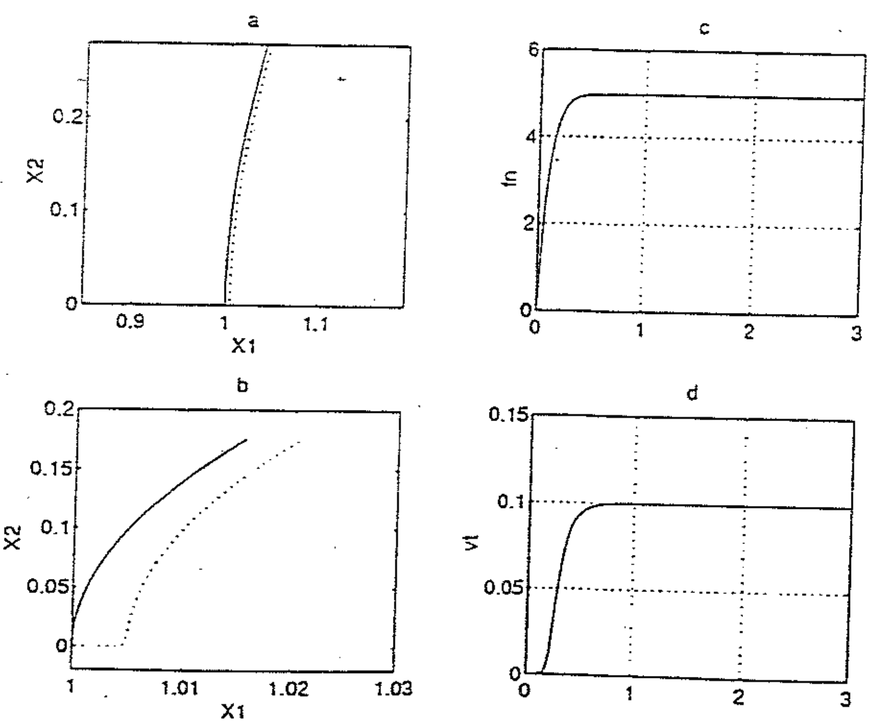

Figure 4: Circumference exploration

while normal force and tangential velocity set points are $f_{dn} = 5N$ and $v_{dt} = 0.1m/s$. Simulation results are shown in fig.2. At the beginning the controller action increases the normal force (fig.2a) while the velocity loop is not yet active (fig.2c) because of the variable structure action (in the initial phase $k_v \simeq 0$ (fig.2d)). When the force error is near zero, velocity loop becomes effective and the tangential velocity approaches to the reference value $0.1m/s$. The surface asperity (fig.3a) generates the discontinuity of the normal force prime derivative (fig.2a), and the control reaction is an inactivation of the velocity loop while recovering reference normal force value. Fig.2b shows the evolution of the first joint torque. In fig.3b, the dashed line inside the object represents the virtual trajectory of ${}^m x$ while the continuous line is the contact point trajectory and reproduces the explored surface. Finally fig.3c-d zoom virtual and contact point trajectory in the initial phase and when the finger meets the surface asperity.

In the second simulation the explored surface is a circumference of radius $R = 1m$ and center in $(x_{1c}, x_{2c}) = (2, 0)m$. Fig.4 summarize the simulation results: fig.4c-d describe the normal force and the tangential velocity evolution, and it can be remarked that the force loop is faster than the velocity one. Dashed line in fig.4a is the virtual trajectory of ${}^m x$ while continuous line is the trajectory reconstructed by the tactile sensor. Finally fig.4b zooms these trajectory in the initial phase. Numerical simulation are performed using SIMULINK software.

6 Conclusions

The problem of controlling force and motion to explore an unknown surface have been investigated. The task is to automatically explore a rigid and unknown surface, by continuous regulation of normal contact force and tangential velocity. Force control guarantees contact stability while velocity loop generates the motion of the fingertip along the object surface.

A controller based on a tactile sensor information has been proposed. Its peculiarity is that the force control has been realized by a model-based computed torque technique and a variable structure controller is used to regulate the interaction between force and velocity loops.

Simulations on a three link planar robot, showing the good performance of the force/velocity controller, have been presented.

Acknowledgement

This work has been supported by CNR funding.

References

[1] N. Hogan, "Impedance control: An approach to manipulation; Part I-Theory; Part II-Implementation; Part III-Applications," ASME J.Dynam. Syst., Measurement Contr., vol 107, 1985.

[2] H.Kazerooni et al., "Robust compliance motion for manipulators; Part I:The fundamental concepts of compliant motions; Part II: Design methods," in Proc. IEEE J.Robotics Automation, vol.RA-2, 1986.

[3] J.H.Salisbury, "Active stiffness control of a manipulator in Cartesian coordinates," in Proc. IEEE Conf. Decision. Contr., Albuquerque, NM, 1980.

[4] G.Hirzinger, "Force feedback problems in robotics," IASTED Symp. on Modelling, Identification and Contr., Davos, 1982.

[5] M.T.Mason, "Compliance and force control for computer-controlled manipulators," IEEE Trans. Syst.,Man,Cyber., vol.SMC-11, 1981.

[6] D.Whitney, "Force feedback control of manipulator fine motions," ASME J.Dynam. Syst., Measurement Contr., 1971.

[7] A.Balestrino and A.Bicchi, "Adaptive Surface Following and Reconstruction Using Intrinsic Tactile Sensing," SIFIR, Zaragoza, Spain, 1989.

[8] L. Cai, A.A. Goldemberg, "A New Approach to Force and Position Control of Robot Manipulators," ICCON, Jerusulem, 1989.

[9] M.H.Raibert and J.J.Craig, " Hybrid position/force control of manipulators," J. Dyn. Syst. Meas., Contr., vol. AC-26, no. 4, 1981.

[10] H.Zhang and R.P.Paul, "Hybrid Control of Robot Manipulators," in Proc.IEEE Int. Conf. on Robotics and Automation, pp. 602-607, 1985.

[11] T.Yabuta, "Nonlinear Basic Stability Concept of the Hybrid Position/Force Control Scheme for Robot Manipulators," IEEE Trans. on Robotics and Automation, vol. 8, no. 5, 1992.
[12] H.Krishanan and N.H.McClamroch, "A New Approach to Position and Contact Force Regulation in Constrained Robot Systems," Proc. IEEE Conf. on Robotics and Automation, pp.1344-1349, 1990.
[13] J.J.E.Slotine and W.Li, "Adaptive Strategies in Constrained Manipulators," Proc. IEEE Conf. Robotics and Automation, pp.595-601, 1987.
[14] R.Carelli and R.Kelly, "An Adaptive Impedance/Force Controller for Robot Manipulators," IEEE Trans. Automat. Contr., vol.AC-36, pp.967-971, 1991
[15] L.Lui et al., "On Adaptive Force/Motion Control of Constrained Robots," in Proc. IECON'89, 1989.
[16] C.Y.Su, T.P.Leung and Q.J.Zhou, "Adaptive Control of Robot Manipulators Under Constrained Motion," in Proc. IEEE Conf. Decision Contr., p.2650, 1990.
[17] N.H.McClamroch and D.Wang, "Feedback Stabilization and Tracking of Constrained Robots," IEEE Trans. Automat. Contr., vol.33, pp419-426, 1988.
[18] M.Aicardi, G.Cannata and G.Casalino, " Application of Learning Techniques in The Hybrid Control of Mechanical Manipulators," Int. Workshop on Intelligent Motion Control, Istanbul, 1990.
[19] D.Jeon and M.Tomizuka, " Learning Hybrid Force and Position Control of Robot Manipulators," in Proc. IEEE Conf. Robotics and Automation, Nice, France, 1992.
[20] V.I. Utkin, "Sliding Modes and Their Applications," Mir:Moskow, 1978.
[21] S.D. Eppinger and W.P. Seering, "Three Dynamic Problems in Robot Force Control," in Proc. IEEE Conf. on Robotics and Automation, 1989.
[22] A.A.Goldemberg, "Analysis of Force Control Based on Linear Models," in Proc. IEEE Conf. on Robotics and Automation, Nice, France, 1992.
[23] J.K.Salisbury and B.Roth "Kinematic and Force Analysis of Articulated Mechanical Hands," ASME Journal of Mechanical Design, 82-DET-13, 1982.
[24] M.R.Cutkosky and I.Kao, "Computing and Controlling the Compliance of a Robotic Hand," in Proc. IEEE Conf. on Robotics and Automation, 1989.
[25] R.P.Paul, "Manipulator Cartesian Path Control," IEEE Trans. Sys. Man and Cyb. SMC-9, pp702-711, 1979.
[26] A.Balestrino, A.Landi, G.Nardi and C.Scali, "Variable Structure PI Control in The Presence of Uncertainty and Saturation", IFAC, Sydney, 1993
[27] A.Bicchi, J.K.Salisbury and D.L.Brock, "Contact Sensing From Force Measurements," Int. Jour. Robot. Res., vol.12, no.3, 1993.